International Society for Rock Mechanics and Rock Engineering
Norwegian Group for Rock Mechanics

ISRM International Symposium
Eurock 2025 – Expanding the Underground Space
Trondheim, Norway, 16-20 June
ISBN 978-82-8208-079-8

Numerical assessment on the influence of Faults in In-situ Stress State Distribution

B. Chaudhary & K.K. Panthi
Norwegian University of Science and Technology, Trondheim, Norway
bikash.chaudhary@ntnu.no

Abstract

Faults within the earth's crust are widespread and formed through prolonged tectonic processes. These faults vary in scale, orientation and degree of lithification. The faults are formed under specific in-situ stress regime predominantly influenced by tectonic stress.

Over time, these stress fields have undergone multiple transformations and superpositions due to various geological processes, resulting in notably complex stress regimes. The spatial distribution of in-situ stresses in faulted areas are often inconsistent and uneven. Reorientation and changes in stress magnitude near fault zones lead to significant local variability in the in-situ stress regime. Large as well as small-scale faults can act as stress concentrators, causing stress to accumulate on adjacent sides of the faults. This concentration results in stress jumps or discontinuities across the faults, leading to abrupt shifts in stress regimes in the fault vicinity.

Tunnels or engineering excavations that intersects or aligned near these structural discontinuities can encounter complex in-situ stress regimes such as abnormal increase or decrease in principal stress values. This complexity is particularly critical for unlined pressure tunnels, where the stability and integrity of the structure may be significantly impacted by the low in-situ stress conditions. This article investigates the impact of faults on the distribution of in-situ stress regime using numerical modeling. The primary objective is to examine how variations in fault/interface stiffness and fault geometry influence stress distribution and also to investigate the integrity of an unlined pressure tunnel/shaft that either crosses or is situated near a fault zone.

Keywords

In-situ stress, Fault zone, Minimum principal stress, Stiffness contrast

1 Introduction

Accurately determining the distribution of the in-situ stress state is essential in any underground projects. As the lengths and burial depths of tunnels and shafts are increasing day by day, encountering complex geological conditions such as faults zones becomes inevitable. These geological features significantly alter the in-situ stress conditions in their vicinity, posing numerous challenges for project design and construction (Basnet & Panthi, 2019).

The complex stress state around fault zones can lead to unexpected stress concentrations, reorientations, and discontinuities (Su & Stephansson, 1999), which must be carefully accounted for to ensure the stability and safety of underground structures. The presence of these discontinuities can profoundly impact the distribution of in-situ stress and may contribute to hydraulic failure of the rock mass, resulting in significant water leakage from unlined pressure tunnels, as demonstrated in a study by Chaudhary & Panthi (2023). Several site measurements indicate that stresses near faults zones exhibit variations in both magnitude and orientation, along with stress discontinuities or jumps across fault planes (Ziegler et al., 2024).

The influence of faults on the present-day stress field in the upper crust has been presented in World Stress Map database (Heidbach et al., 2018). However, a systematic investigation quantifying the magnitude and extent of this impact as a function of fault in-situ parameter remains largely unexplored. Reiter et al., (2024), in their work presented that most in-situ stress changes attributed to faults may originate from different sources such as density and strength contrasts. In-situ stress rotations and variations in magnitude have been documented globally in boreholes intersecting fault zones (Cui et al., 2014; Hickman and Zoback, 2004). Observations indicate considerable variability with some faults exhibit stress rotations of up to 90° while others show significantly smaller rotations or no rotation at all (Yamada and Shibanuma, 2015). This observed variability prompts a fundamental question: which major parameters govern in-situ stress variation, and how sensitive are these parameters to changes in fault zone properties and surrounding conditions.

To address this question, this article aims at developing a series of generic three-dimensional (3D) geo-mechanical models to systematically analyze the influence of fault zones on the in-situ stress distribution along tunnel-fault zone intersection. The major focus is made on the minimum principal stress perturbation is figured out using the 3D generic model by varying the stiffness properties of the fault zones. Furthermore, the extent/distance of the stress perturbations within the surrounding rock mass of the fault zone over various stiffness contracts is also examined via numerical model.

2 3D Model configuration and input parameters.

The primary objective of this study is to develop and analyze a generic three-dimensional (3D) numerical model to investigate the influence of a fault zone on the in-situ stress distribution at the intersection of a tunnel and the fault zone. The 3D model is designed to represent a simplified yet realistic geological scenario where the interaction between the fault zone and surrounding rock mass can be observed under regional stress conditions.

The 3D model as represented in Figure 1, consists of three primary components: (1) a 20m thick fault zone with dip angle of 15 º, (2) the surrounding concentric rock mass of 50m following the tunnel periphery, and (3) a larger encompassing rock mass block (1000mx1000mx500m) where regional stresses are applied. The tunnel and fault zone interaction are modelled at the center of the domain, where the tunnel axis intersects the fault zone. Appropriate boundary conditions are assigned to the outer boundaries of the 3D model to replicate regional stress states.

To simplify the mechanical properties of the rock mass, the model assumes a homogeneous, isotropic rock medium with a Young's modulus of 40 GPa, Poisson's ratio of 0.25, and a density of 2750 kg/m³. The fault zone (E_{fault}), however, is modeled with varying stiffness relative to the surrounding rock mass ($E_{rockmass}$), introducing stiffness contrasts from 1 to 0.1 to assess their effect on in-situ stress redistribution along the intersection.

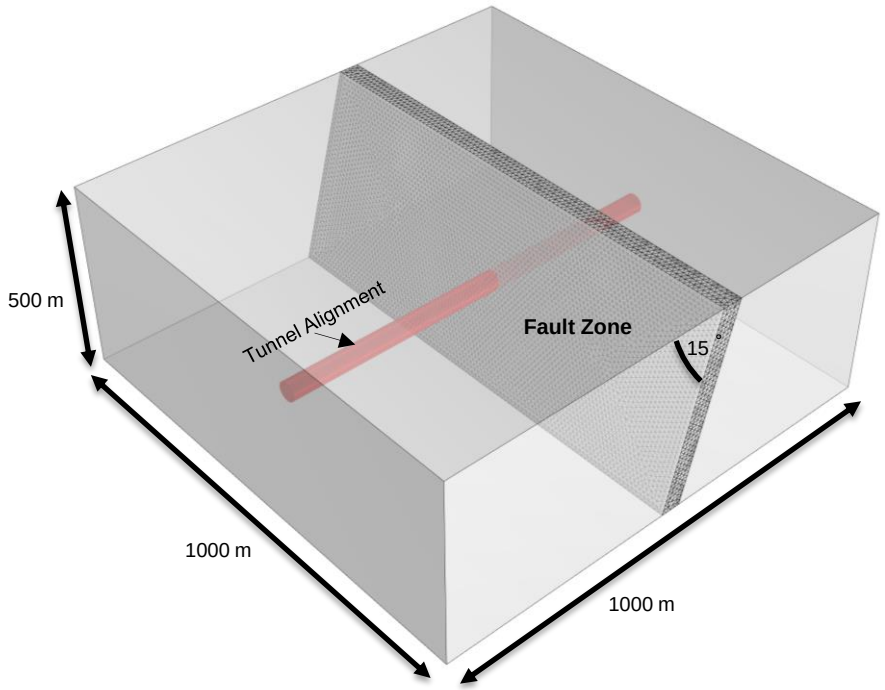

Figure 1: A generic 3D model with model extent

3 Methodology and Simulation Process

After the 3D block geometry as illustrated in Figure 1 is defined, 3D tetrahedral volume grids of different sizes are created after the discretization of the 3D block (Figure 2), rock mass parameters are assigned along with the boundary conditions. The boundary faces of north, south, east, west, and bottom are prevented from normal displacement by fixing corresponding velocities to zero values.

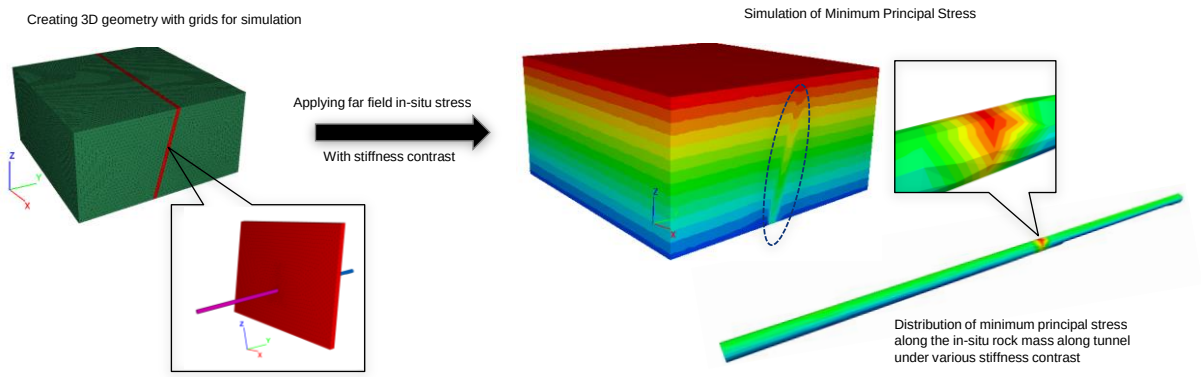

Figure 2: 3D model illustrating rock mass block, fault zone volume grids (left) and 3D numerical model for minimum principal stress assessment (right)

After the mesh discretization, relevant rock mass parameters, including elastic modulus, Poisson's ratio, and density, were assigned to the model elements. Boundary conditions were applied to the model to simulate realistic constraints: the north, south, east, west, and bottom boundary faces were fixed against normal displacement by setting their corresponding velocities to zero, ensuring no movement across these boundaries.

To simulate the initial stress field, the model was initialized with gravity stress and gravity induced stresses using Poisson's ratio. The system was allowed to reach equilibrium, ensuring convergence under initial conditions. After equilibrium was established, maximum and minimum horizontal stress values of 15 MPa and 10 MPa, respectively, were applied to reflect realistic far-field in-situ stress conditions. Initially, the model was run with the input parameters, assuming a stiffness contrast between the fault (E_{fault}) and the surrounding rock mass ($E_{rockmass}$) of 1. The resulting in-situ stress from this model was then compared with a model where the stiffness of the fault zone was systematically varied from

1.0 (matching the surrounding rock mass) to 0.1 (one-tenth the stiffness of the surrounding rock), enabling a comparative analysis under different stiffness contrasts.

4 Analysis Results and discussion

4.1 Minimum principal stress perturbation over the stiffness contrasts of fault zone

Within the fault zone area, the minimum principal stress (S3) perturbation is significant as shown in Figure 3a. It is clearly represented in Figure 3b that the reduction of S3 is more significant with low stiffness of fault zone. This condition occurs when the elastic modulus of the fault zone (E_{fault}) is much lower than that of the surrounding rock mass ($E_{rockmass}$), leading to a localized drop in stress magnitudes. The fault zone, acting as a mechanically weaker region, absorbs and redistributes the stress into adjacent areas, causing stress relaxation within the intersection. Such stress redistribution can result in potential instability, particularly in unlined pressure tunnel where the minimum principle stress around the tunnel periphery must be examined.

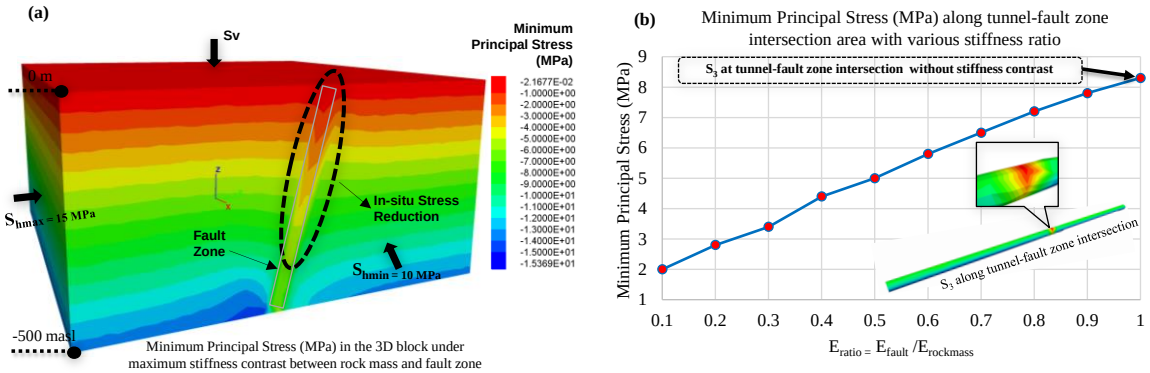

Figure 3: Reduction of minimum principal stress over the stiffness contrast of the fault zone

Figure 3b provides a quantitative relationship between the stiffness ratio Eratio=Efault/Erockmass and the corresponding minimum principal stress (S3) along the tunnel-fault intersection. At very low stiffness ratios (Eratio=0.1), S3 is minimized (~2 MPa), indicating significant stress reduction due to the weak mechanical response of the fault zone. As the stiffness ratio increases, the fault zone behaves more like the surrounding rock mass, and S3 rises steadily. This linear trend culminates at Eratio=1.0, where the fault zone has no stiffness contrast with the surrounding rock, and S3 approaches its maximum value (~9 MPa). This behavior emphasizes the critical role that stiffness contrast plays in controlling stress redistribution, with weak fault zones leading to stress relaxation and stiffer zones contributing to stress concentration around the excavation.

Furthermore, the results presented in this analysis underscore the importance of thorough geo-mechanical characterization of fault zones during the early stages of tunnel planning. Laboratory testing and in-situ measurements of the elastic modulus and other rock mass properties can help determine the stiffness ratio and predict stress redistribution patterns. Numerical modeling and simulation can further enhance the understanding of stress behavior around tunnel-fault intersections, allowing engineers to optimize excavation methods and support designs. These insights are particularly valuable in regions with complex geological conditions, where fault zones are unavoidable and pose significant risks to the stability of underground structures.

4.2 Influence zone of the fault with respect to stiffness contrast

The analysis result of the influence/disturbed zone along the tunnel-fault intersection has been presented in Figure 4. It provides a comprehensive analysis of how the stiffness contrast between a fault zone and the surrounding rock mass influences the extent of the disturbed zone when a tunnel intersects the fault. On the left, the graph demonstrates the relationship between the stiffness contrast and the fault influence distance, which is measured in meters. At a very low stiffness ratio (Eratio=0.1), the fault influence distance is approximately 70 meters, highlighting a maximum disturbance due to the substantial difference in stiffness. As the stiffness contrast reduces (i.e., as Eratio increases), the fault zone influence distance decreases progressively. This trend continues until Eratio=1.0, where the stiffness of the fault

zone and surrounding rock mass are identical, and the influence distance reduces to zero, implying no significant disturbance.

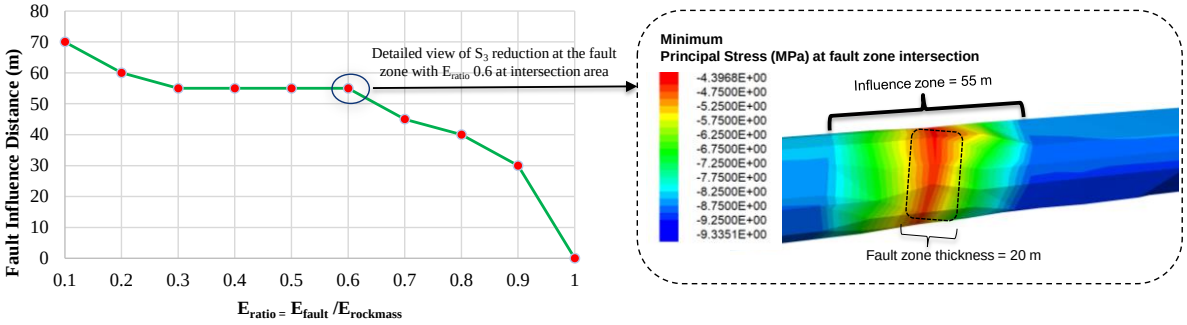

Figure 4: Influence zone of the tunnel-fault zone with respect to the stiffness contrast between the fault zone and the surrounding rock mass.

To further analyze the stress redistribution at intermediate stiffness contrasts, a detailed view at E_{ratio}=0.6 is provided (right side of Figure 4). The stress contour plot on the right shows the distribution of the minimum principal stress (S3) around the fault zone and the tunnel. The stress contours indicate that the fault zone thickness is 20 meters, while the overall disturbed region, or influence zone, extends to 55 meters. This observation suggests that when there is a moderate stiffness contrast, the stress redistribution propagates through a broader region around the tunnel. The stress reduction near the fault-tunnel intersection is particularly notable, as shown by the red and orange contours in the plot, which represent zones of higher stress concentration.

The results collectively highlight the critical role of stiffness contrast in determining the mechanical behavior of the tunnel-fault interaction. When the fault zone stiffness is low relative to the surrounding rock mass, it acts as a weak region, causing significant stress concentration and disturbance to propagate over a larger area. This occurs because the softer fault material cannot adequately support the loads, leading to stress redistribution into the surrounding stiffer rock. Conversely, as the stiffness contrast diminishes, the fault zone behaves more similarly to the surrounding rock, limiting the extent of the disturbance. Such findings are essential in tunnel design and stability assessments, as they emphasize the need for considering fault stiffness in determining the influence length and stress response in rock masses intersected by faults.

4.3 In-situ Stress concentration along the fault zone under various stiffness contrast

The minimum principal stress is seen to be concentrated against the dip direction of the fault zone as represented in Figure 5. The relationship between stress concentration along the tunnel-fault zone intersection and the stiffness contrast ratio between the fault zone and the surrounding rock mass is shown in Figure 5a. As E_{ratio} decreases from 1.0 (indicating equal stiffness) to 0.1 (representing a significant stiffness contrast where the fault zone is much softer than the surrounding rock), the stress concentration increases progressively.

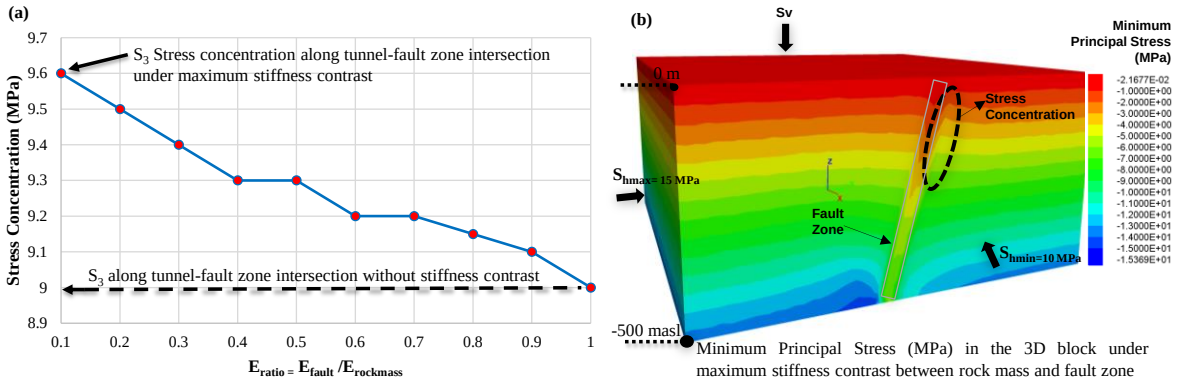

Figure 5: In-situ Stress concentration along the fault zone under various stiffness contrast

When there is no stiffness contrast (E_{ratio} = 1.0), the stress concentration remains constant at approximately 9 MPa, as indicated by the horizontal dashed line. However, under maximum stiffness contrast (E_{ratio} = 0.1), the stress concentration reaches its peak value of approximately 9.6 MPa. This trend highlights the significant influence of stiffness contrast on stress distribution at the tunnel-fault intersection. A softer fault zone relative to the surrounding rock mass concentrates stress more intensively, as the weaker material cannot effectively redistribute the applied stresses. Consequently, the stress concentration deviates from the baseline level observed when stiffness is uniform. These findings emphasize the importance of considering stiffness contrast during tunnel design, particularly in regions with soft geological structures embedded in harder rock masses, as such conditions may necessitate additional measures to manage elevated stress concentrations and ensure long-term structural stability.

5 Conclusion

From this generic numerical model one can figure out that, at low stiffness ratios (e.g., E_{ratio}=0.1), the fault zone is significantly weaker compared to the surrounding rock, leading to a substantial reduction in S_3 along the tunnel-fault intersection. The 3D model visually illustrates this phenomenon, where the fault zone acts as a mechanical discontinuity, inducing localized stress relaxation (in-situ stress reduction). This results in significant stress redistribution into the surrounding rock mass.

The faults zones with significant stiffness contrasts may act as pathway for water leakage since it may create low confinement of minimum principal stress in the rock mass. Once the internal water pressure is above the minimum principal stress, hydraulic failure of the rock mass may occur. Understanding stress reduction near weak faults can help prevent unanticipated failures and improve implementation of unlined pressure tunnel/ shaft especially in the planning phase.

Thus, creating a 3D numerical model with site specific input parameters can help to enhance the understanding of in-situ stress distribution along the fault zone. Calibrating such model with help of measured in-situ stress data will further enhance the credibility of the model and can be used to simulate stress redistribution around tunnels intersecting fault zones for real cases. By incorporating stiffness contrast into geotechnical models, engineers can optimize tunnel alignments, excavation methods, and support designs to minimize risks associated with stress redistribution especially for unlined pressure tunnel where the confinement of the minimum principal stress is most critical.

References

Basnet, C. B., & Panthi, K. K. (2019). Evaluation on the Minimum Principal Stress State and Potential Hydraulic Jacking from the Shotcrete-Lined Pressure Tunnel: A Case from Nepal. Rock Mechanics and Rock Engineering, 52(7), 2377–2399.

Chaudhary, B., Panthi, K. K., & Trinh, N. Q. (2023, October 9). Assessment on the In-Situ Rock Stress Condition Along an Unlined Pressure Tunnel/Shaft of a Norwegian Hydropower Project Using Numerical Modeling. 15th ISRM Congress.

Heidbach, O., Rajabi, M., Cui, X., Fuchs, K., Müller, B., Reinecker, J., Reiter, K., Tingay, M., Wenzel, F., Xie, F., Ziegler, M. O., Zoback, M.-L., & Zoback, M. (2018). The World Stress Map database release 2016: Crustal stress pattern across scales. Tectonophysics, 744, 484–498.

Hickman, S., & Zoback, M. (2004). Stress orientations and magnitudes in the SAFOD pilot hole. Geophysical Research Letters, 31(15).

Reiter, K., Heidbach, O., & Ziegler, M. O. (2024). Impact of faults on the remote stress state. Solid Earth, 15(2), 305–327. https://doi.org/10.5194/se-15-305-2024

Su, S., & Stephansson, O. (1999). Effect of a fault on in situ stresses studied by the distinct element method. International Journal of Rock Mechanics and Mining Sciences, 36(8), 1051–1056.

Yamada, Y., & Shibanuma, J. (2015). Small-scale stress fluctuations in borehole breakouts and their implication in identifying potential active faults around the seismogenic megasplay fault, Nankai Trough, SW Japan. Earth, Planets and Space, 67(1), 17.

Ziegler, M. O., Seithel, R., Niederhuber, T., Heidbach, O., Kohl, T., Müller, B., Rajabi, M., Reiter, K., & Röckel, L. (2024). Stress state at faults: The influence of rock stiffness contrast, stress orientation, and ratio. Solid Earth, 15(8), 1047–1063.